

- 270-4, 270-5, National Bureau of Standards, U.S. Department of Commerce, Washington, DC (1968, 1969).
19. M. W. Chase, C. A. Davies, J. R. Downey, D. J. Frurip, R. A. McDonald, and A. N. Syverud, "JANAF Thermochemical Tables," 3rd ed., in *J. Phys. Chem. Ref. Data*, **14**, Suppl. No. 1 (1985).
 20. *Gmelin Handbuch der Anorganischen Chemie, Seltenerelemente*, No. 39, Teil C4a, Springer, Berlin (1982).
 21. I. Barin and O. Knacke, "Thermochemical Properties of Inorganic Substances," Springer, Berlin (1973).
 22. O. Kubaschewski, E. L. Evans, and C. B. Alcock, "Metallurgical Thermochemistry," 4th ed., Pergamon Press, Ltd., Oxford (1967).
 23. I. Barin, O. Knacke, and O. Kubaschewski, "Thermochemical Properties of Inorganic Substances," Suppl., Springer, Berlin (1977).
 24. *Gmelin Handbuch der Anorganischen Chemie, Seltenerelemente*, No. 39, Teil C6, Springer, Berlin (1978).
 25. *Ibid.*, No. 39, Teil C5, Springer, Berlin (1977).
 26. M. W. Chase, J. L. Curnutt, A. T. Hu, H. Prophet, A. N. Syverud, and L. C. Walker, "JANAF Thermochemical Tables," 1974 Suppl., in *J. Phys. Chem. Ref. Data*, **3**, 311 (1974).
 27. M. W. Chase, J. L. Curnutt, H. Prophet, R. A. McDonald, and A. N. Syverud, "JANAF Thermochemical Tables," 1975 Suppl., in *J. Phys. Chem. Ref. Data*, **4**, 1 (1975).
 28. D. R. Stull and H. Prophet, "JANAF Thermochemical Tables," 2nd ed., in *NBS Ref. Data Ser. 37*, National Bureau of Standards, U.S. Department of Commerce, Washington, DC (1971).
 29. M. Guido, G. Gigli, and G. Balducci, *J. Chem. Phys.*, **57**, 3731 (1972).
 30. M. Guido, G. Balducci, G. Gigli, and M. Spoliti, *ibid.*, **55**, 4566 (1971).
 31. T. E. Joyce and E. J. Rolinski, *J. Phys. Chem.*, **76**, 2310 (1972).
 32. J. Carre, H. Pham, and M. Rolin, *Bull. Soc. Chim. Fr.*, **7**, 2322 (1969).
 33. J. Karpinski, E. Kaldis, and S. Rusiecki, *J. Less-Common Met.*, **150**, 207 (1989).
 34. L. R. Morris, D. C. Sonnenberger, and R. J. Thorn, *Inorg. Chem.*, **27**, 2106 (1988).

A Reflectometric Study of the Reaction between Si and WF₆ during W-LPCVD on Si and of the Renucleation during the H₂ Reduction of WF₆

J. Holleman, A. Hasper, and J. Middelhoek¹

University of Twente, 7500 AE Enschede, The Netherlands

ABSTRACT

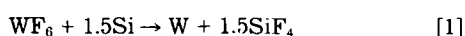
The formation of W through the reduction of WF₆ by Si is monitored *in situ* using a wavelength adjustable reflectometer. The reflectance-time relation can be understood and modeled by assuming island growth and a statistical distribution of the island thickness. The model is supported by SEM and Auger observations. The effect of surface layers like native oxides or a plasma treatment on the inhomogeneous Si consumption by the reaction between Si and WF₆ (gouging) and its effect on the reflectance-time relation are understood. The model is also applicable in the case of renucleation during the H₂ reduction of WF₆. A renucleation step consists of the deposition of Si from SiH₄ followed by the Si consumption by WF₆. A renucleation step reduces the surface roughening which occurs during the H₂ reduction process.

W can be grown selectively on Si through the reduction of WF₆ with Si, H₂, and SiH₄ (1-3). The Si reduction reaction was found to be self-limiting (2). The thickness of the self-limiting layer is determined among others, by the presence and thickness of a native oxide layer (2, 4) and other surface treatments (5). Others (6, 7) found that the W thickness is not self-limiting under certain conditions. The proposed reason for self-limitation (4, 6, 8, 9) was the coalescence of W islands that grow out of nuclei.

Reflectometry has proven to be a valuable tool to monitor the initial reaction between WF₆ and Si (10). It can be helpful in the study of the mechanism of W-layer growth and the study of the influence of surface layers on gouging and encroachment.

Experimental

The study of the initial W formation via the reaction



was performed at a wafer temperature of 400°C on 3 in. p-type 10 Ω cm (100) wafers in a single-wafer coldwall reactor with a load lock and chuck heating (see Fig. 1). The purity of the WF₆ was 99.999%. Wafers were cleaned in 100% HNO₃, then boiled in 70% HNO₃, rinsed in DI water, and prior to deposition, dipped in a 1% HF solution in order to remove the oxide. After the dip the wafers were rinsed in DI water. These wafers will be referred to as "HF dip." Some wafers were boiled again in 70% HNO₃ for 20 min after the dip in order to form a reproducible oxide. Such

wafers will be referred to as "no HF dip." The influence of plasma treatments was studied as well. Details are mentioned under Results and Discussion.

The gas flow and pressure settings during the deposition were: WF₆ flow = 10 sccm, Ar flow = 1000 sccm, total pressure = 1.0 torr.

The renucleation experiments were performed during the H₂ reduction of WF₆ at 400°C



W layers formed according to reaction [2] have a large surface roughness (10, 11). A renucleation step can improve the surface roughness (10). The renucleation sequence consists of: (1) W deposition proceeds according to reaction [2]; (2) WF₆ is switched off. The reactor is purged for 10 s; (3) SiH₄ is switched on. Si deposits according to reaction [3]; (4) SiH₄ is switched off. The reactor is purged for 10 s; and (5) WF₆ is switched on again. Reaction [1] consumes the deposited Si



Although this reaction normally takes place at about 600°C, the fresh W surface apparently catalyzes the decomposition of SiH₄ (12) so that it readily decomposes at the temperature where reaction [2] takes place (400°C). Flow and pressure setting during reactions [2] and [3] are: WF₆ flow = 20 sccm, H₂ flow = 1000 sccm, Ar flow = 190 sccm, and total pressure = 1 torr; and SiH₄ flow = 50 sccm, H₂ flow = 1000 sccm, Ar flow = 190 sccm, and total pressure = 1 torr, respectively. In order to avoid reflection from the quartz window the reflectance is measured at near normal

¹ Deceased.

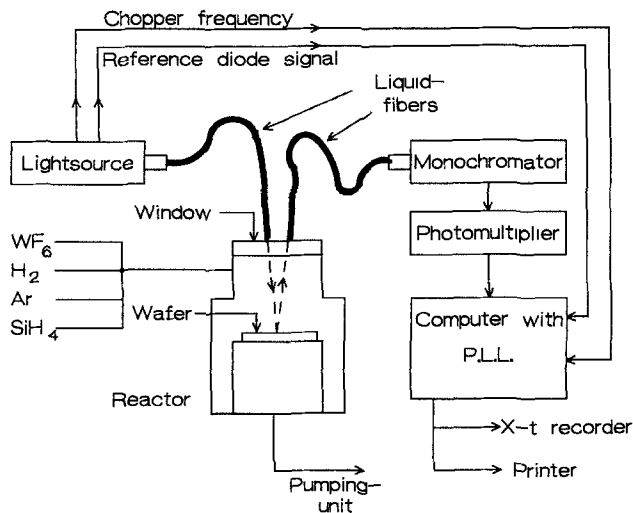


Fig. 1. Schematic drawing of the reactor and reflectometer setup

incidence through a large quartz window by a reflectometer system, as shown in Fig. 1. Reflectance in this paper is presented as a unit normalized to the Si reflectance. The solid angle of acceptance of the instrument was about 0.03 sr, which is sufficiently small to avoid the measurement of incoherently reflected light of the wavelength range studied in this paper. Reflectance measurements were performed at a wavelength (λ) of $\lambda = 400$ and 600 nm, respectively.

Theory and Model

The reflectance (R) of a multilayer stack is given by

$$R = (\mathbf{E}_r/\mathbf{E}_i)^2 \quad [4]$$

where \mathbf{E}_r and \mathbf{E}_i are the amplitudes of reflected and incident electric field vector at the first interface respectively. R can be computed by a matrix method (13, 14).

The amplitude ratio in [4] is given by

$$\mathbf{E}_r/\mathbf{E}_i = \frac{am_{11} + bm_{12} - cm_{12} - m_{22}}{am_{11} + bm_{12} + cm_{21} + m_{22}} \quad [5]$$

where $a = Y_0/Y_{k+1}$, $b = Y_0$, $c = 1/Y_{k+1}$ and

$$\mathbf{M} = \begin{bmatrix} m_{11} & m_{12} \\ m_{21} & m_{22} \end{bmatrix} = \prod_{k=1}^k \mathbf{M}_v$$

\mathbf{M}_v is called the characteristic matrix of the v^{th} layer and is given by

$$\mathbf{M}_v = \begin{bmatrix} \cos \phi_v & j \sin \phi_v Y_v \\ j Y_v \sin \phi_v & \cos \phi_v \end{bmatrix}$$

where $\phi = (2\pi/\lambda) \cdot n_v \cdot h_v \cdot \cos \theta_v$, λ is the wavelength, n_v the refractive index, h_v the layer thickness, θ_v angle of incidence, and Y_v the admittance; subscript v indicates the v^{th} layer.

If we have more multilayer stacks side by side on the same surface, including height differences, the reflectance can be calculated from the Fresnel-Kirchhoff diffraction equation (18). For the plane wave approximation and for nonmultiple reflections on the surface we can follow the procedure as presented by Porteus (17), except that the Fresnel reflection now appears under the integral sign because it varies over the surface.

$$R = (\iint \rho(\mathbf{r}) \mathbf{k} \cdot \mathbf{n}(\mathbf{r}) \cdot \mathbf{N} \cdot \mathbf{n}(\mathbf{r}) \exp -i\mathbf{k} \cdot \mathbf{r} \, dx dy)^2 \quad [6]$$

Where $\rho(\mathbf{r})$ is the local Fresnel reflection, \mathbf{n} is the local normal, \mathbf{r} is a position vector, $\mathbf{k} = \mathbf{k}_i - \mathbf{k}_d$ is the difference between the propagation vector of the incident and diffracted beam, and \mathbf{N} is the surface normal.

When the diffracted and incident beam are taken normal (\mathbf{N}) to the surface and when we consider the surface as an

ensemble of discrete multilayer stacks, we may write Eq. [6] as

$$R = (\sum F_i \rho_i \exp j\delta_i)^2 \quad [7]$$

where F_i is the fraction of surface covered by layer stack i , ρ_i is the Fresnel reflection of layer stack i , and $\delta_i = 4\pi h_i/\lambda$, with h_i the height difference between the surface of layer stack i and some reference surface, in general the mean surface level.

Equation [7] can be used to calculate the reflectance of a rough surface on which a film is growing. According to Ohlidal *et al.* (15), when both the air-film and the film-substrate interface have their own characteristic roughness, such a film is called a general film. When the film grows in islands we just have a special case of the general film. In our case islands of W are formed, whose lateral and vertical growth rates have a statistical distribution.

We developed a code that computes the reflectance of a surface with a maximum of m multilayer stacks, see Fig. 2. Each stack can be built up of a maximum of n layers. The thickness of each layer as well as the surface fraction covered by each stack can be varied. The code can be used to calculate the reflectance of a surface covered with W islands of various size and thickness.

Equation [7] is applicable when the Kirchhoff boundary conditions are satisfied (18). This is the case (15) when

$$4\pi r_c \cos \eta \gg \lambda \quad [8]$$

where r_c is the radius of the curvature of the surface irregularity, and η is the angle between the wave vector of the incident beam and the local normal. Even when Eq. [8] is not strictly fulfilled, the Fresnel-Kirchhoff equation has been applied successfully, as is demonstrated by the good agreement between this approach and measurements (10, 11, 16, 17, 19, 20).

In our model the Fresnel-Kirchhoff equation is approached by Eq. [7], considering the surface fraction covered with islands within the same thickness range as one stack. In the case of nucleation the model does not take into account the density and diameter of the islands but only the surface fraction covered by the islands. The thickness of the W layer when the surface closes, *i.e.*, no free substrate is visible anymore, is given by

$$thc = ad \cdot vgr/lgr \quad [9]$$

where thc is the average thickness at closing, vgr is the average vertical growth rate, ad is the average lateral distance between nuclei, and lgr is the average lateral growth rate. For the case that $vgr = lgr$ we get $thc = ad$.

W grows at the expense of Si . At temperatures below 400°C SiF_4 is the main by-product. At higher temperatures SiF_2 becomes the main by-product (21). According to reaction [1], 1.5 molecule of Si is consumed for the formation of 1 molecule of W . Taking the molecular volume ratio into account, the volume of Si that is etched is twice the amount of deposited W (22).

It was shown by Wong *et al.* (7) that W islands growing on Si consume Si from underneath the island and in the lateral direction, causing voids. Schematically the observations by Wong *et al.* (7) and Green *et al.* (8) are presented in Fig. 3, which is the basis of our model for calculating the reflectance. The surface can be divided in three regions: (i)

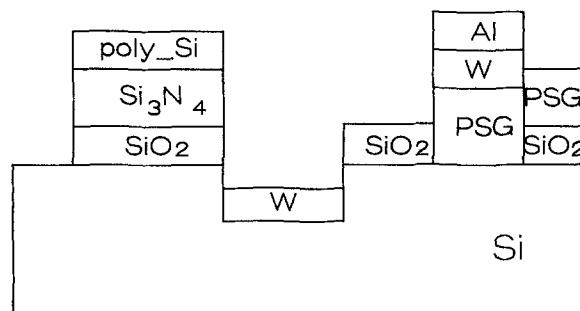


Fig. 2. Example of a surface with more multilayer stacks

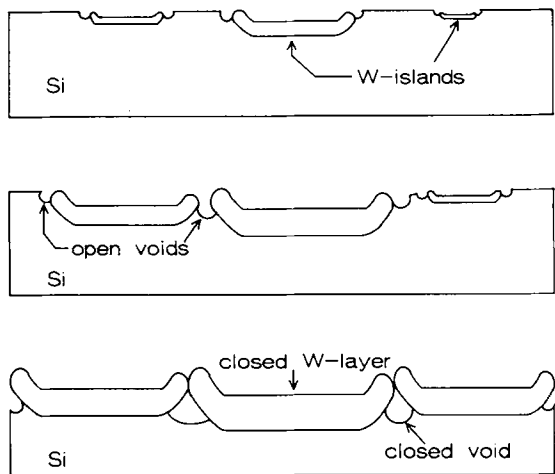


Fig. 3. Schematic representation of the W island growth: (a) initial island formation, (b) islands close, and (c) after growth.

Si fraction, (ii) W fraction, and (iii) void fraction. The W surface (region 2) is divided in subfractions through which a statistical variation of the island growth rate is included in the reflectance calculation. The W surface fraction F_{wab} with grain thickness between a and b can be found by integration of the grain thickness density function $f(G)$, where G is the grain thickness

$$F_{wab} = \int_a^b f(G)dG \quad [10]$$

The average thickness of $d_{F_{wab}}$ in the substack F_{wab} is given by

$$d_{F_{wab}} = \int_a^b f(G) G dG / \int_a^b f(G) dG \quad [11]$$

The simulation of the reflectance is performed in two stages: (i) Islands grow vertically and laterally until the surface closes; region 1 decreases from 1 to 0 (see Fig. 3b). (ii) After the surface is closed all grains increase uniformly in thickness, probably by diffusion of Si via the grain boundary voids represented by surface 3 until the grain boundaries become clogged leading to self-limitation of the layer thickness (see Fig. 3c). A similar model as proposed by Kuiper *et al.* (6) assumes an initial vertical growth followed by lateral growth only.

Results and Discussion

The average thickness of the W layer during the Si reduction of WF_6 is calculated from the weight gain using 19.3 g/cm^3 for the W-specific gravity. These measurements were performed for both HF dip and no HF dip wafers, see Fig. 4. Auger depth profiles at various stages are presented in Fig. 5. A SEM photograph of the early stage of growth in the no HF dip case is presented in Fig. 6 and clearly shows that the growth proceeds through island growth; Fig. 6 corresponds to the Auger profile of Fig. 5c. Similar observations were done by Wong *et al.* (7) that showed that the island's surface is below the Si surface. From the depth profile (Fig. 5c and d) we may conclude that the islands in the early stage of growth already have a thickness close to the final thickness. This conclusion may be drawn from the fact that about 120 min are required to sputter through the W islands covering about 20% of the surface (Fig. 5c) and about the same time is needed for the W layer in Fig. 5d.

In the case of HF-dipped wafers, such islands were not observed by SEM because the shortest reaction time of 2 s already yields a closed surface that shows no Si in the Auger spectrum (see Fig. 5a). However, after little sputtering of about 1.5 nm the Si becomes visible, indicating that the layer just became closed at 2 s. The reflectance of the corresponding layers was measured at 400 and 600 nm, re-

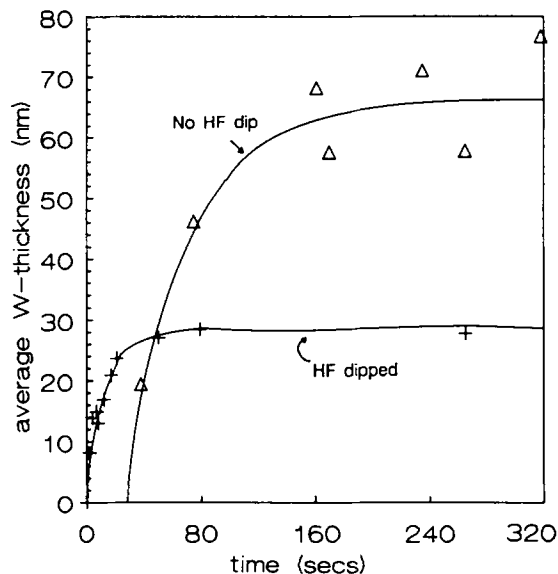


Fig. 4. Average W thickness formed during reaction [1]

spectively, and is presented in Fig. 7a and b for HF-dipped and nondipped wafers. The reflectance was simulated for various conditions using the data of Fig. 4. The results are presented in Fig. 8a for HF-dipped wafers and in Fig. 8b for no HF dip wafers.

The reflectance was calculated for three cases with the following assumptions: (1) layer-by-layer growth (van der

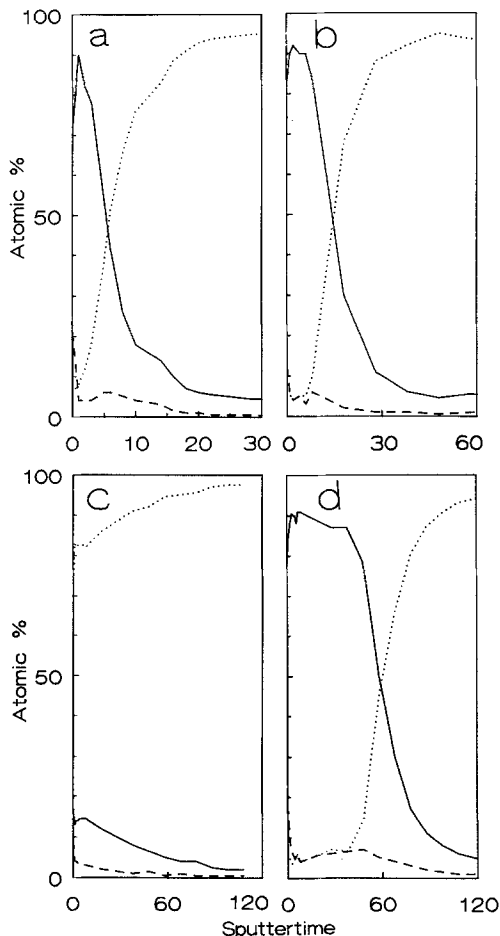


Fig. 5. Auger depth profiles: (a) HF-dipped wafers, average W thickness 8 nm; (b) HF-dipped wafers, average W thickness 28 nm; (c) no HF dip, average W thickness 20 nm; and (d) no HF dip, average W thickness 65 nm.

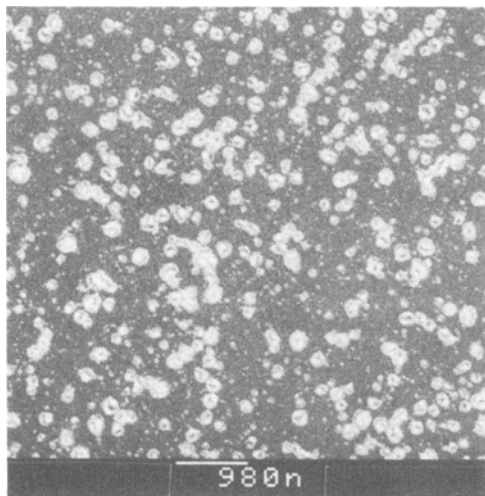


Fig. 6. W-island formation during the early stage of W growth ($t = 20$ s) on wafers with no HF dip.

Merwe growth) is assumed. (2) Island growth was assumed; the grain thickness density function is assumed to be a delta function. (3) Island growth was assumed; the grain thickness density function is assumed to be a Gaussian function with $3\sigma = t_{hc}$ (see Eq. [9]).

For HF-dipped wafers it is assumed that the layer closes at an average thickness of 8 nm as was found by Auger; for the no HF dip case the layers close at an average thickness of 48 nm. During the process of closing a constant ratio was assumed between the vertical and lateral growth rate; this means that at a 50% coverage, the thickness also is 50% of its thickness at closing.

As was proposed by Kuiper *et al.* (6) and also based on our own observation presented in Fig. 5c and d, one can also assume a fast vertical growth rate till the grains have the thickness which is observed when the layers close. The calculated reflectance-time relation, however, shows no basic difference in such a case. In our simulation we assumed that 90% of the W is formed by vertical consumption of Si and 10% by lateral consumption. The lateral consumption creates a 20% void density; the effective W density then becomes 80% of the bulk value, which is a reasonable assumption (6, 7). Others, however, found lower values for the average W density (23-25). After closing of the layer, a uniform increase of thickness with 20 nm was assumed, which is in agreement with the observation by Auger sputter profiling. The uniform growth proceeds probably by surface diffusion of Si in the boundary void.

The diffusion of WF_6 or Si through the grains is not likely since such a mechanism would result in a continuous

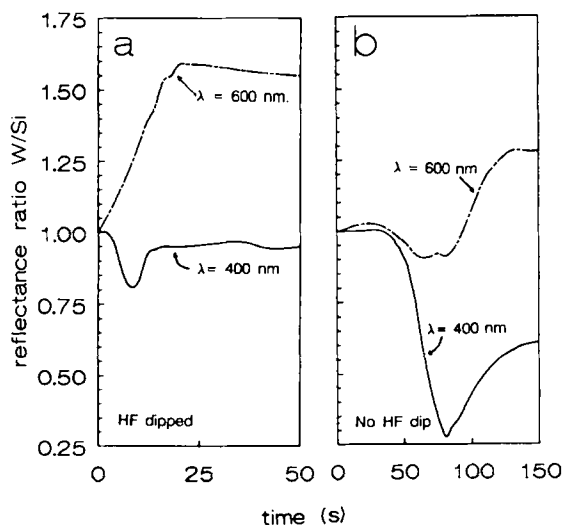


Fig. 7. Reflectance measurement during W deposition

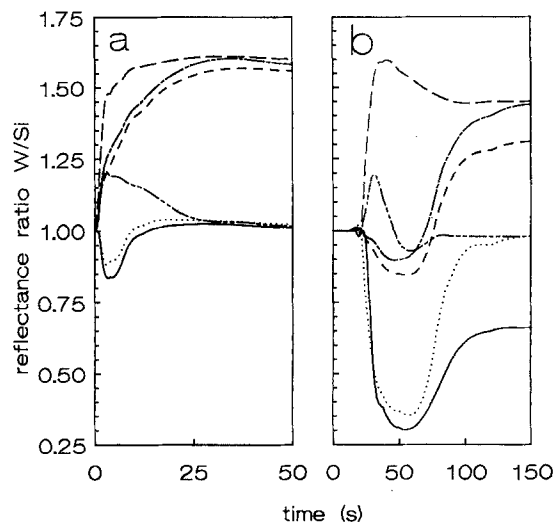


Fig. 8. Simulation of the reflectance: (a) HF-dipped, and (b) no HF dip. 1. Layer-by-layer growth is assumed: — $\lambda = 400$ nm; — $\lambda = 600$ nm. 2. Island growth is assumed with a delta density function of the grain thickness distribution: $\lambda = 400$ nm; - - - $\lambda = 600$ nm. 3. Island growth is assumed with a Gaussian density function of the grain thickness distribution: — $\lambda = 400$ nm; — $\lambda = 600$ nm.

growth. Diffusion of WF_6 through voids has been proposed by Wood and Collins (26). In view of our model, however, a surface diffusion of Si to the surface through the boundary voids or pore may explain the observations. WF_6 may react at the inlet of the pore; any WF_6 diffusing into the pore then reacting will cause the pore to become clogged. Once the pore is closed the growth stops creating a closed void. Surface diffusion of WF_6 has been shown not to be of great importance in the modeling of step coverage in W low-pressure chemical vapor deposition (27).

If we compare the measurement with the calculation we may draw the conclusion that the reflectance modeling during W growth by means of reaction [1] assuming island growth is realistic. The conclusion is supported by SEM and Auger measurements.

The reflectance for a layer-by-layer growth model strongly disagrees with the measurement. Assuming a delta density function for the thickness distribution is not realistic for wafers that received no HF dip, because this would result in flat layers, whereas in SEM observation rough layers are observed (2, 7) and the measured final reflection would be higher. A Gaussian distribution is more realistic. Such a distribution also explains why the W/Si interface is much rougher than the W surface (2), and it explains why the final reflectance for the thick W layer formed on wafers with no HF dip is lower than the theoretical value for a smooth layer. Also, with Rutherford backscattering (RBS) grain thickness variations are observed on similar samples (28). A Gaussian distribution of the grain thickness can explain their observed RBS profile (29).

The reflectance simulations compared to measurements for HF-dipped wafers cannot discriminate between a Gaussian or delta function because the surface roughness involved with the thin layer is too small to make any decision about the density function. It is evident, however, also in the HF-dipped case that island growth predicts the reflectance-time relation rather than the layer-by-layer growth model which would yield quite a different dependence. The dip at the onset of growth is due to diffraction. The shift on the time axes between measurements and calculation is probably due to a small difference in native oxide thickness between the series of the weight measurement of Fig. 4 on which the calculations are based, and the reflectance measurements presented in Fig. 7. The weight measurements and reflectance measurements are from two different series. A small variation in native oxide thickness can produce large delay effects.

For the reflectance calculations bulk values were used (30). The calculations and measurements are in good agreement, so we may conclude that the grains in our experiments have bulk characteristics at least in the top layer. The voids are not visible to the beam, which is in agreement with our model.

The influence of other surface treatments was studied as well. Wafers were subjected to one or more of the following treatments: (1) Standard cleaning as described under Experimental including the dip in 1% HF solution. (2) Boiling in 70% HNO₃ for 5 min. (3) O₂ plasma treatment performed at 1 torr with 100W power in a barrel reactor. (4) CHF₃ plasma treatment in a RIE reactor at 40 mtorr, power density = 0.5 W/cm² and dc bias = 300 V. (5) Plasma treatment in a gas mixture composed of 90% CF₄ and 10% O₂ in a RIE reactor at 40 mtorr, power density = 0.5 W/cm² and dc bias = 300 V. (6) Dip in 1% HF. (7) *In situ* NF₃ plasma afterglow treatment. The reflectance was measured at λ = 400 nm because this wavelength is more sensitive to the effect of gouging than higher wavelengths. The results of the experiments are presented in Fig. 9.

If we consider the minimum of the reflectance as a measure for the degree of gouging, which is a reasonable assumption considering the agreement between the previously presented model and the results, we may draw the following conclusions from Fig. 9:

Boiling in 70% HNO₃, also for short times, forms an oxide responsible for gouging (treatment 1 + 2). The thickness of the oxide formed by HNO₃ was found to be 1.8 nm by ellipsometry. O₂ plasma treatments for short times (5 s) form an oxide of about 1.5 nm, which causes gouging (treatment 1 + 3, 5 s). When the plasma treatment is performed longer than 1 min, the oxide formed is about 2.1 nm (treatment 1 + 3, 1 min) and so dense that no W is deposited at all within 10 min.

In a CHF₃ plasma a thin layer of 4 nm is formed composed of C, F, and O as was found by x-ray photoelectron

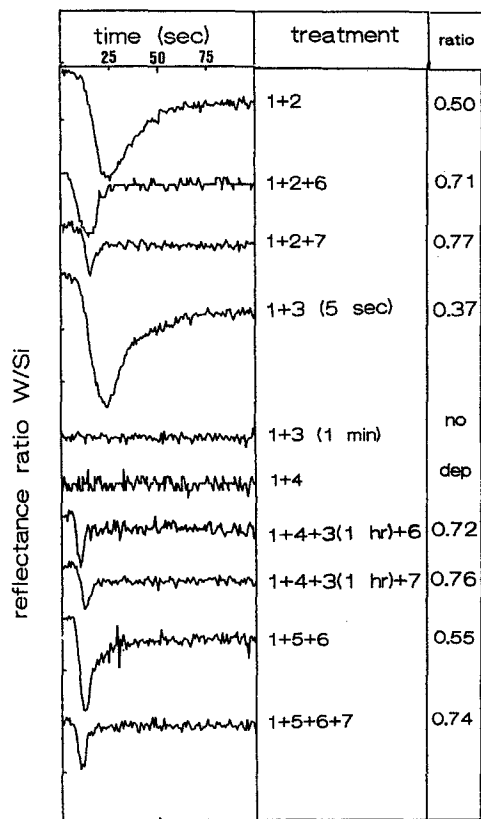


Fig. 9. The reflectance-time relation measured at λ = 400 nm after various surface treatments. The curves are displaced vertically for clarity. The starting point of each curve corresponds to the Si reflectance. The meaning of the surface treatments as presented in the first column is explained in the text. The second column presents the minimum reflectance.

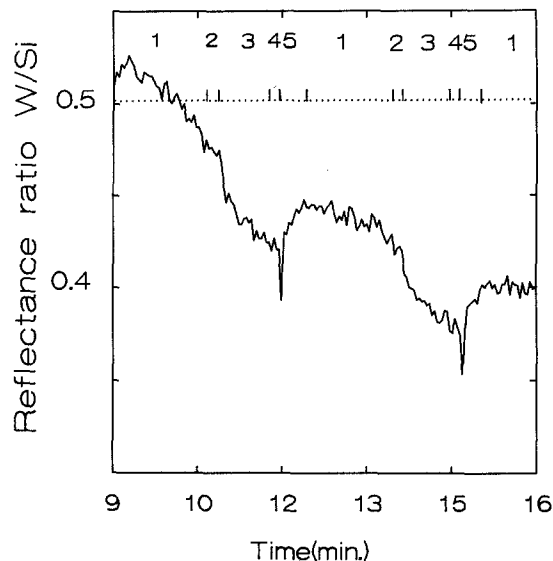


Fig. 10. Reflectance measurement during two renucleation sequences: step 1 H₂ reduction reaction, step 2 WF₆ off, step 3 SiH₄ on, step 4 SiH₄ off, step 5 WF₆ on.

spectroscopy (XPS) (treatment 1 + 4). This layer does not increase in thickness for longer plasma treatment times and could not be removed by a 1% HF dip. The layer hinders the formation of any W. A CF₄ + O₂ plasma also forms a surface layer, although to a lesser extent, that cannot be removed by a 1% HF dip and which is responsible for gouging (treatment 1 + 5 + 6).

The layers formed by the CHF₃ plasma and CF₄ plasma can be removed by an O₂ plasma followed by either an HF dip or an *in situ* NF₃ plasma treatment (treatment 1 + 4 + 3 + 6, 1 + 4 + 3 + 7, 1 + 5 + 6 + 7). In general, the minimum reflectance found after a 1% HF dip is lower than after an NF₃ *in situ* cleaning, possibly because an oxide of about 0.6 nm is formed between the HF dip and the loading into the reactor.

Renucleation.—When W is deposited according to reaction [2], the surface becomes rough. The surface roughness was found to be independent of deposition temperature (10, 11) and the root mean square (rms) roughness is about 7% of the layer thickness. A renucleation sequence as mentioned under Experimental can improve the roughness (10). In step 1 of the sequence (see Fig. 10) W grows according to reaction [2]. The reflectance decreases due to an increasing roughness. In step 3 the reflectance decreases strongly due to the formation of Si by reaction [3]. The Si thickness can be calculated from the reflectance change by means of Eq. [4] and was found to be ≈2 nm thick assuming the optical constants of crystalline Si. Auger measurements by Schmitz *et al.* (12) confirm the Si formation and thickness. The Si thickness saturates as can be seen from Fig. 10, probably because the formed Si screens the catalyzing action of the W. When the WF₆ is switched on again in step 5 the Si is consumed by reaction [1]. The sharp decrease in reflectance at the onset of renucleation cannot be understood in terms of the Fresnel-Kirchhoff diffraction equation. Height differences during the nucleation step can never be large enough to explain the phenomenon, because the Si layer is only 2 nm thick and the renucleated W layer will not be more than 1 nm. A breakdown of the Kirchhoff boundary conditions is very realistic, since the radius of the initial nuclei will not satisfy Eq. [8]. Together with this, a nucleus density much larger than in the HF-dipped case must be assumed, which is realistic since the freshly formed Si is free of any oxide.

Conclusions

The reflectance change during W formation via the LPCVD reaction of WF₆ with Si can be modeled by assuming nucleus formation followed by lateral and vertical growth that results in island formation. The nucleus density is so high in the case of HF-dipped wafers that the sur-

face already closes at an average thickness of 8 nm. Growth then proceeds through diffusion at boundary voids and stops, probably due to clogging of the pores. The nuclei can grow in thickness as long as the surface is open; therefore, the final thickness in the dipped case is much lower than in the nondipped case, because the dipped wafer surface closes sooner due to a higher nucleus density.

The reflectance minimum measured at $\lambda = 400$ nm is a good measure for the degree of gouging caused by surface layers. The reflectance measurement during a renucleation step is a good tool to get insight into the renucleation process.

Acknowledgment

This work forms part of the "Innovatief Onderzoeks Programma IC technologie" (Innovating Research Program for IC Technology) and was made possible by the financial support from the Netherlands Ministry of Economic Affairs.

Manuscript submitted April 27, 1990; revised manuscript received Oct. 8, 1990.

University of Twente assisted in meeting the publication costs of this article.

REFERENCES

- W. A. Bryant, *This Journal*, **125**, 1534 (1978).
- E. K. Broadbent and C. L. Ramiller, *ibid.*, **131**, 1427 (1984).
- R. F. Foster, S. Tseng, and L. Lane, in "Proceedings of the 1987 Workshop on Tungsten and Other Refractory Metals for VLSI Applications III," V. A. Wells, Editor, p. 69, Materials Research Society, Pittsburgh, PA (1988).
- H. H. Busta and C. H. Tang, *This Journal*, **133**, 1195 (1986).
- W. T. Stacy, E. K. Broadbent, and M. H. Norcott, *This Journal*, **132**, 444 (1985).
- A. E. T. Kuiper, M. F. C. Willemsen, and J. E. J. Schmitz, *Appl. Surf. Sci.*, **38**, 338 (1989).
- M. Wong, N. Kobayashi, R. Browning, D. Paine, and K. C. Saraswat, *This Journal*, **134**, 2339 (1987).
- M. L. Green, Y. S. Ali, T. Boone, B. A. Davidson, L. C. Feldman, and S. Nakahora, in "Proceedings of the 1986 Workshop on Tungsten and Other Refractory Metals for VLSI Applications II," E. K. Broadbent, Editor, p. 85, Materials Research Society, Pittsburgh, PA (1987).
- R. S. Blewer, V. A. Wells, and M. E. Tracy, in "Proceedings of the 1985 Workshop on Tungsten and Other Refractory Metals for VLSI Applications," R. S. Blewer, Editor, p. 407, Materials Research Society, Pittsburgh, PA (1986).
- J. Holleman, A. Hasper, and J. Middelhoek, in "Chemical Vapor Deposition of Refractory Metals and Ceramics," T. M. Besman and B. M. Galois, Editors, p. 107, Materials Research Society Symposium, Boston, MA, Nov. 29-Dec. 1, 1989.
- T. I. Kamins, D. R. Bradbury, T. R. Cass, S. S. Laderman, and G. A. Reid, *This Journal*, **133**, 2555 (1986).
- J. E. J. Schmitz, M. J. Buiting, and R. C. Ellwanger, in "Proceedings of the 1988 Workshop on Tungsten and Other Refractory Metals for VLSI Applications IV," R. S. Blewer and C. M. McConica, Editors, p. 27, Materials Research Society, Pittsburgh, PA (1989).
- A. Vasicek, "Optics of Thin Films," North Holland, Amsterdam (1960).
- C. v. d. Laan and H. J. Frankena, *Appl. Optics*, **17**, 538 (1978).
- I. Ohlidal, K. Navratil, and F. Lukes, *J. Opt. Soc. Am.*, **61**, 1630 (1971).
- H. E. Bennet and J. O. Porteus, *ibid.*, **51**, 123 (1961).
- J. O. Porteus, *ibid.*, **53**, 1394 (1963).
- M. Born and E. Wolf, "Principles of Optics," 5th ed., Chap. 8, Pergamon Press, Ltd., Oxford (1975).
- H. E. Bennet, *J. Opt. Soc. Am.*, **53**, 1389 (1963).
- K. L. Chiang, C. J. Dell'Oca, and F. N. Schwettmann, *This Journal*, **126**, 2267 (1979).
- M. L. Yu, B. N. Eldridge, and R. V. Joshi, in "Proceedings of the 1988 Workshop on Tungsten and Other Refractory Metals for VLSI Applications IV," R. S. Blewer and C. M. McConica, Editors, p. 221, Materials Research Society, Pittsburgh, PA (1989).
- M. L. Green and R. A. Levy, *This Journal*, **132**, 1243 (1985).
- J. Wood, *Vacuum*, **38**, 683 (1988).
- M. L. Green, Y. S. Ali, T. Boone, B. A. Davidson, L. C. Feldman, and S. Nakahara, in "Multilevel Metallization, Interconnection, and Contact Technologies," L. B. Rothman and T. Herndon, Editors, PV 87-4, The Electrochemical Society Softbound Proceedings Series, Pennington, NJ (1987).
- H. L. Park, C. D. Park, and J. S. Chun, *Thin Solid Films*, **166**, 37 (1988).
- J. Wood and R. Collins, *Appl. Surf. Sci.*, **38**, 359 (1989).
- A. Hasper, J. Holleman, J. Middelhoek, and C. R. Kleijn, in "Proceedings of the 1989 Workshop on Tungsten and Other Advanced Metals for VLSI/ULSI Applications V," S. S. Wong and S. Furukawa, Editors, p. 127, Materials Research Society, Pittsburgh, PA (1990).
- A. J. P. Van Maaren, R. L. Krans, E. De Haas, and W. C. Sinke, *Appl. Surf. Sci.*, **38**, 386 (1989).
- R. L. Krans, Private communication.
- "Handbook of Optical Constants of Solids," E. D. Palik, Editor, Academic Press, Inc., New York (1985).